DIRAC ELECTRON IN GAPPED GRAPHENE UNDER EXPONENTIALLY DECAYING MAGNETIC FIELD

Le Thi Hoa[1], Tran Ngoc Bich[1], Nguyen Ngoc Hieu[2,3], Le Thi Ngoc Tu[4], and Huynh Vinh Phuc[4*]

[1]Physics Department, University of Education, Hue University, Vietnam

[2]Institute of Research and Development, Duy Tan University, Vietnam

[3]Faculty of Natural Sciences, Duy Tan University, Vietnam

[4]Faculty of Natural Sciences Teacher Education, Dong Thap University, Vietnam

[*]Corresponding author: Huynh Vinh Phuc, Email: hvphuc@dthu.edu.vn

Article history

Received: 26/01/2021; Received in revised form: 02/4/2021; Accepted: 22/4/2021

Abstract

In this work, we present a Dirac electron in gapped graphene under the exponentially decaying magnetic field. Solving Dirac-Weyl equations, we obtain exact expressions of the eigenfunctions and their corresponding eigenvalues. The probability density and current distributions are also investigated in detail. The results are compared to those in the gapless graphene as well as in the gapped graphene in the presence of a uniform magnetic field.

Keywords: *Dirac-Weyl equations, exponentially decaying magnetic field, gapped graphene*.

ĐIỆN TỬ DIRAC TRONG GRAPHENE CÓ VÙNG CẤM HỮU HẠN DƯỚI TÁC DỤNG CỦA TỪ TRƯỜNG GIẢM THEO HÀM MŨ

Lê Thị Hóa[1], Trần Ngọc Bích[1], Nguyễn Ngọc Hiếu[2,3], Lê Thị Ngọc Tú[4] và Huỳnh Vĩnh Phúc[4*]

[1]Khoa Vật lý, Trường Đại học Sư phạm, Đại học Huế, Việt Nam

[2]Viện Nghiên cứu và Phát triển, Trường Đại học Duy Tân, Việt Nam

[3]Khoa Khoa học Tự nhiên, Trường Đại học Duy Tân, Việt Nam

[4]Khoa Sư phạm Khoa học tự nhiên, Trường Đại học Đồng Tháp, Việt Nam

[*]Tác giả liên hệ: Huỳnh Vĩnh Phúc, Email: hvphuc@dthu.edu.vn

Lịch sử bài báo

Ngày nhận: 26/01/2021; Ngày nhận chỉnh sửa: 02/4/2021; Ngày duyệt đăng: 22/4/2021

Tóm tắt

Trong công trình này, chúng tôi xét hệ điện tử Dirac trong graphene có vùng cấm hữu hạn dưới tác dụng của từ trường giảm theo hàm mũ. Giải các phương trình Dirac-Weyl, chúng tôi thu được biểu thức chính xác cho các hàm sóng và năng lượng tương ứng. Chúng tôi cũng khảo sát mật độ xác xuất và mật độ dòng xác suất. Các kết quả được so sánh với trường hợp hệ graphene không có vùng cấm cũng như đối với hệ có vùng cấm hữu hạn khi có mặt từ trường đều.

Từ khóa: *Phương trình Dirac-Weyl, từ trường giảm theo hàm mũ, graphene có vùng cấm hữu hạn.*

DOI: https://doi.org/10.52714/dthu.11.5.2022.978

Cite: Le, T. H., Tran, N. B., Nguyen, N. H., Le, T. N. T., & Huynh, V. P. (2022). Dirac electron in gapped graphene under exponentially decaying magnetic field. *Dong Thap University Journal of Science, 11*(5), 35-40. https://doi.org/10.52714/dthu.11.5.2022.978.

1. Introduction

In the past few decades, interest in studying graphene, a two-dimensional (2D) layer of graphite, has developed speedily caused by its extraordinary electronic and optical properties as well as its potential applications in optical-electronic devices (Novoselov et al., 2005). The most important characteristic of graphene is the massless Dirac nature feature of its electron. This special characteristic of Dirac electron in graphene led to the anomalous Landau level structure in the presence of a uniform magnetic field, which emerges the half-integer quantum Hall effect (Novoselov et al., 2005) as one of the most important fields in quantum physics. This stimulated a lot of theoretical studies interest in Dirac electron in the presence of uniform as well as in non-uniform magnetic fields (Ghosh, 2008; Kuru et al., 2009; Wang & Jin, 2013, Eshghi & Mehraban, 2017). In these works, the Dirac-Weyl equation for a massless electron is investigated to find the exact solutions using the technique of supersymmetric (SUSY) quantum mechanics (Cooper et al., 1995). Recently, this technique has been used successfully to study the unique Landau-level structure of monolayer black phosphorus under a non-uniform magnetic field (Wang et al., 2019). Although this method has been applied successfully to solve the Dirac-Weyl equations in the gapless 2D system, the corresponding word for the gapped 2D system is calling for investigation.

In this work, we use the SUSY method to find the analytical solutions of the Dirac-Weyl equations for the Dirac electron in gapped graphene in the presence of an exponentially decaying magnetic field. The behavior of the discrete Landau level structure, the eigenfunctions, the probability, and current densities have also been discussed in detail.

2. Dirac-Weyl equation

Considering a graphene sheet oriented in the (*xy*)-plane under a perpendicular magnetic field $\vec{B}(x,y)=(0,0,B(x))$, with (Ghosh, 2008)

$$B(x)=B_0e^{-x/\lambda} \tag{1}$$

is exponentially decaying in the *x*-direction where λ is the penetration depth of the magnetic field. The vector potential in the Landau gauge is chosen so that $\vec{A}(x,y)=(0,A_y(x),0)$, where $A_y(x)=-B_0\lambda(e^{-x/\lambda}-1)$. The Hamiltonian of the massless electron near the Dirac point can be described by a two-component Dirac-Weyl equation (Jiang et al., 2010, Krstajić & Vasilopoulos, 2012)

$$H_0=v_F(\tau\sigma_x\pi_x+\sigma_y\pi_y)+\Delta\sigma_z, \tag{2}$$

where $v_F\simeq10^6$ m/s is the Fermi velocity, $\tau=\pm1$ refers to the valley index (for K and K'), σ_i denote the Pauli matrices $(i=x,y,z)$, $\Delta=26.5$ meV is the band-gap (Krstajić & Vasilopoulos, 2012), $\vec{\pi}=\vec{p}+e\vec{A}$ is the canonical momentum with $\vec{p}=-i\hbar\vec{\nabla}$ being the normal momentum. The time-independent Dirac-Weyl equation is

$$v_F[\tau\sigma_x(p_x+eA_x)+\sigma_y(p_y+eA_y)+\Delta\sigma_z]\Psi(x,y)=E\Psi(x,y), \tag{3}$$

where $\Psi(x,y)=(e^{ik_yy}/\sqrt{L_y})\Psi(x)$ is the two-component eigenfunction with

$$\Psi(x)=\begin{pmatrix}\psi_+(x)\\ i\psi_-(x)\end{pmatrix} \tag{4}$$

being the eigenfunction in the x-direction, and *i* the units of imaginary numbers. From Eq. (3), we can obtain two coupled equations for $\psi_+(x)$ and $\psi_-(x)$ as follows

$$\hbar v_F(\tau\partial_x+W)\psi_-=(E-\Delta)\psi_+, \tag{5}$$

$$\hbar v_F(-\tau\partial_x+W)\psi_+=(E+\Delta)\psi_-. \tag{6}$$

Equations (5) and (6) are the Dirac-Weyl equations for massless electron in a gapped graphene system with

$$W=k_y+\left(\frac{e}{\hbar}\right)A_y=k_y+\frac{eB_0\lambda^2}{\hbar}\left(1-e^{-x/\lambda}\right) \tag{7}$$

being the super potential function (Midya & Fernandez, 2014). Using Eqs. (5) and (6) we will get Schrödinger-like decoupled equations for $\psi_+(x)$ and $\psi_-(x)$ as follows

$$H_\pm\psi_\pm=(E^2-\Delta^2)\psi_\pm, \tag{8}$$

where

$$H_\pm=-(\hbar v_F)^2\partial_x^2+V_\pm(x) \tag{9}$$

are the Hamiltonian supersymmetric partners. In Eq. (9) we have denoted

$$V_{\pm}(x) = (\hbar v_F)^2 \left[W^2 \pm \tau(\partial_x W) \right] \quad (10)$$

as the effective potentials.

3. The eigenfunctions and eigenvalues

To obtain the solutions of Eq. (8), following the suggestions from previous works (Handrich, 2005; Ghosh, 2008), we use the dimensionless variables

$$\xi(x) = \frac{eB_0\lambda^2}{\hbar} e^{-x/\lambda} = \left[\frac{\lambda}{\alpha_c(x_0)} \right]^2, \quad (11)$$

$$\xi_0 = \lambda \left(k_y + \frac{eB_0\lambda}{\hbar} \right) \equiv \xi(x_0) = \left[\frac{\lambda}{\alpha_c(x_0)} \right]^2, \quad (12)$$

where $\alpha_c(x) = \left[\hbar / eB(x) \right]^{1/2}$ is the magnetic length. Then, Eq. (8) becomes

$$\left[\partial_\xi^2 + \frac{1}{\xi}\partial_\xi - \frac{\beta^2}{\xi^2} + \frac{2\xi_0 \mp \tau}{\xi} - 1 \right] \psi_\pm = 0, \quad (13)$$

where we have denoted

$$\beta^2 = \xi_0^2 - \frac{\lambda^2 (E^2 - \Delta^2)}{(\hbar v_F)^2}. \quad (14)$$

The solutions of Eq. (13) are found under the form

$$\psi_\pm(\xi) = \xi^\beta e^{-\xi} w_\pm(\xi), \quad (15)$$

which are suggested from the asymptotic condition (Handrich, 2005). Inserting Eq. (15) into Eq. (13), we will get the following equation for $w(z = 2\xi)$

$$\left[z\partial_z^2 + (\gamma - z)\partial_z - \alpha_\pm \right] w_\pm(z) = 0. \quad (16)$$

Here, $\gamma = 2\beta + 1$, and $\alpha_\pm = \beta - \xi_0 + 1/2 \pm \tau/2$. The solutions of Eq. (16) are the confluent hypergeometric functions as follows (Ghosh, 2008)

$$w_\pm(z) = {}_1F_1(\alpha_\pm; \gamma, z). \quad (17)$$

Due to the requirement of renormalizability of the solutions, the term $\alpha_\pm$ has to be a negative integer, i.e., $\alpha_\pm = -\nu$ with $\nu = 0,1,2,\ldots$ Using this relation, we have

$$\beta = \xi_0 - \left(\nu + \frac{1}{2} \pm \frac{\tau}{2} \right). \quad (18)$$

From Eqs. (14) and (18) we get the following expression for the energy

$$E_n = p\sqrt{\left(\frac{\hbar v_F}{\lambda} \right)^2 n(2\xi_0 - n) + \Delta^2}, \quad (19)$$

where $p = \pm 1$ is for the conduction and valence bands, respectively.

The corresponding eigenfunction in Eq. (4) can be written

$$\Psi_n(x) = \begin{pmatrix} A_{n,p}\psi_{n-1}(x) \\ iB_{n,p}\psi_n(x) \end{pmatrix}, \quad (20)$$

Here the normalization constants are

$$A_{n,p} = \sqrt{\frac{pE_n + \Delta}{2pE_n}}, \quad B_{n,p} = p\sqrt{\frac{pE_n - \Delta}{2pE_n}}, \quad (21)$$

and the component eigenfunctions

$$\psi_n(x) = \sqrt{\frac{(2\beta)\Gamma(n+1)}{\bar{\lambda}\alpha_c(x_0)\Gamma(n+2\beta+1)}} (2\xi_0)^\beta e^{-\beta X/\bar{\lambda}} \times e^{-\xi_0 e^{-X/\bar{\lambda}}} L_n^{2\beta}\left(2\xi_0 e^{-X/\bar{\lambda}} \right), \quad (21)$$

where we have denoted $\bar{\lambda} = \lambda / \alpha_c(x_0) = 1/\sqrt{\xi_0}$, $X = (x - x_0)/\alpha_c(x_0)$, $\Gamma(n)$ is the Gamma functions, and $L_n^{2\beta}(x)$ are the *n*-order Laguerre polynomials.

4. Discussions

In this section, we will evaluate numerically the above results in more detail. Using the relation $\xi = \xi_0 e^{-\bar{\lambda}X}$, the effective potentials in Eq. (10) can be written as

$$\begin{aligned} V_\pm(x) &= \left(\hbar v_F \right)^2 \left[\left(\lambda\xi_0 - \lambda\xi \right)^2 \pm \lambda^2 \xi \right] \\ &= \frac{\left(\hbar v_F \right)^2}{\left[\alpha_c(x_0) \right]^2} \left[\xi_0 \left(1 - e^{-X/\bar{\lambda}} \right)^2 \pm \tau e^{-X/\bar{\lambda}} \right] \\ &= \frac{1}{2} \left[\hbar\omega_c(x_0) \right]^2 \left[\xi_0 \left(1 - e^{-X/\bar{\lambda}} \right)^2 \pm \tau e^{-X/\bar{\lambda}} \right] \end{aligned} \quad (22)$$

which has the same form as that obtained in the gapless graphene (Ghosh, 2008). This implies that the effective potential is independent of the structure of the system.

For the strong inhomogeneity magnetic field (small λ), the strong asymmetry of the effective potentials is clearer as shown in Figure 1(a). At very large values of *x*, both $V_\pm(x)$ reach their saturated value of $\xi_0 \left[\hbar\omega_c(x_0) \right]^2 / 2$. Indeed, from Eq. (22) we have

$$\lim_{X\to\infty} V_{\pm}(x) = V(X\to\infty) = \frac{\xi_0}{2}\left[\hbar\omega_c(x_0)\right]^2. \quad (23)$$

This saturated value of $V_{\pm}(x)$ is displayed by the purple line in Figure 1(a).

For the weak inhomogeneity magnetic field (large λ), we have

$$\lim_{\lambda\to\infty} V_{\pm}(x) = \frac{1}{2}\left[\hbar\omega_c(x_0)\right]^2 (X^2 \pm \tau). \quad (24)$$

In this case, the effective potentials in the gapped graphene are degraded into the harmonic potentials, i.e., almost symmetric around the $X = 0$ point as shown in Figure 1(b), being the same as that obtained in the gapless graphene (Ghosh, 2008). It is clear that the expression of the magnetic field in Eq. (1) will reduce to the case of the uniform magnetic field when the inhomogeneity magnetic field is weak. It means

$$\lim_{\lambda\to\infty} B(x) = \lim_{\lambda\to\infty} B_0 e^{-x/\lambda} = B_0. \quad (25)$$

For the energy spectrum shown in Eq. (19), we also have

$$\lim_{\lambda\to\infty} E_n = p\sqrt{n(\hbar\omega_c)^2 + \Delta^2}. \quad (26)$$

It means that the energy spectrum is also reduced to that in the case of the uniform magnetic field (Krstajić & Vasilopoulos, 2012).

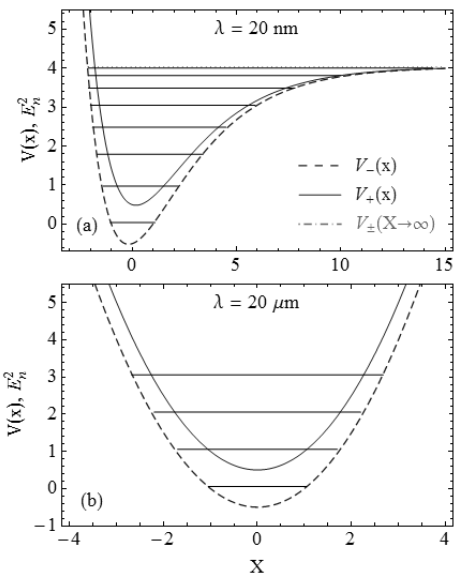

Figure 1. The dependence of the $V_{\pm}(x)$ and E_n (in units of $\left[\hbar\omega_c(x_0)\right]^2$) on the X-parameter for two values of λ: (a) for λ= 20 nm, and (b) for λ = 20 μm. The results are evaluated at B = 10 T and k_y = 2 x 10^8/m

For the number of energy levels, unlike in the uniform magnetic field case (Krstajić & Vasilopoulos, 2012), the number of energy levels in the inhomogeneity one is limited. The total number of energy levels not including the zero-one, $N_{\max}$, can be found from the condition that $E_n^2 < V_{\pm}(X\to\infty)$ (Ghosh, 2008), which leads to

$$N_{\max} < \xi_0 - s\sqrt{2\xi_0}, \text{ with } s = \Delta/\hbar\omega_c(x_0). \quad (27)$$

For the values of the parameters used in Figure 1(a), i.e., λ= 20 nm, B = 10 T, and k_y = 2 x 10^8/m we have $N_{\max} < 7.3$, leading to the fact that there are (7+1) energy levels in the energy spectrum, which is shown clearly in Figure 1(a).

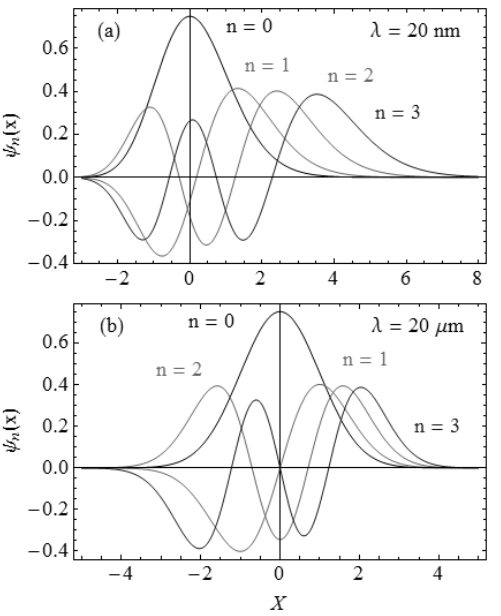

Figure 2. The component eigenfunctions $\psi_n(x)$ for some first Landau levels (in units of $\left[\alpha_c(x_0)\right]^{-1/2}$) versus the X-parameter for two values of λ: (a) for λ= 20 nm, and (b) for λ = 20 μm. The results are evaluated at B = 10 T and k_y = 2 x 10^8/m

In Figure 2, we show the dependence of the X-parameter at two different values of λ. It can be seen that when the inhomogeneity magnetic field is strong, equivalent to the small value of λ, the eigenfunctions are strongly asymmetric (see Figure 2(a)) as is expected from the asymmetry of the effective potentials shown in Figure 1(a). Meanwhile, when the penetration depth of the magnetic field is large, the eigenfunctions are symmetric around the $X = 0$ point, which is the

result of the symmetric behavior of the effective potentials when the λ has large values.

The probability density distributions are calculated as follows

$$\rho_n(x) = \Psi_n^\dagger(x)\Psi_n(x), \quad (28)$$

where the eigenfunctions are shown in Eq. (20), and $\Psi_n^\dagger(x)$ denotes the Hermite conjugation of $\Psi_n(x)$. The probability density distributions for some first Landau levels is presented in Figure 3 for two cases of strong and weak inhomogeneity magnetic fields. We can see from the figure that the probability density distribution for the case of $n = 0$ is symmetrical and reaches its maximum value at the point $X = 0$ point. This implies that the probability of finding the Dirac electron, in the case of $n = 0$, will have its maximum value at point $X = 0$ point. Besides, we also note that the symmetrical/ asymmetrical behavior of the $\rho_0(x)/\rho_{1,2,3}(x)$ is from the symmetrical/ asymmetrical behavior of the $\psi_0(x)/\psi_{1,2,3}(x)$ as shown in Fig. 2. Due to the asymmetry/ symmetry of the effective potentials, the probability density distributions display their asymmetric/ symmetric behaviors in the small/large values of λ. These results are in good agreement with those obtained in gapless graphene (Ghosh, 2008).

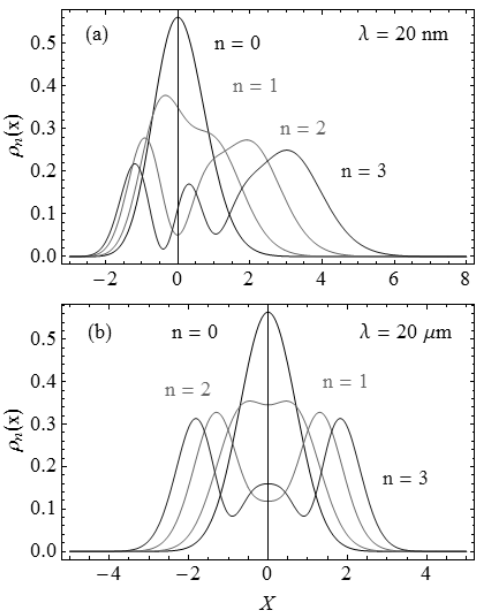

Figure 3. The same as Figure 2 but for the probability density distributions $\rho_n(x)$ (in units of $\left[L_y\alpha_c(x_0)\right]^{-1/2}$)

The probability current density, a mathematical quantity describing the flow of probability in terms of probability per unit time per unit area, is calculated as follows

$$J_n(x) = ev_F\Psi_n^\dagger(x)\sigma_y\Psi_n(x)$$
$$= ev_F(\psi_{n-1}^*\psi_n + \psi_n^*\psi_{n-1}). \quad (29)$$

Here the component eigenfunctions are shown in Eq. (21). We can see that $J_0(x) = 0$, implying that the zero-state does not contribute to the probability current density. Due to the asymmetry of the effective potentials in the case of a strong inhomogeneity magnetic field, the probability current density shifts to the right-hand side with the increase of the Landau level index (see Figure 4(a)). In the case of a weak inhomogeneity magnetic field, the probability current density tends to be symmetrical around point $X = 0$ point. Similar to the case of the probability density distributions as shown in Fig. 3, the asymmetrical behavior of the probability current density for $n = 1, 2, 3$ shown in Fig. 4 is also from the asymmetrical behavior of the eigenfunctions as shown in Fig. 2.

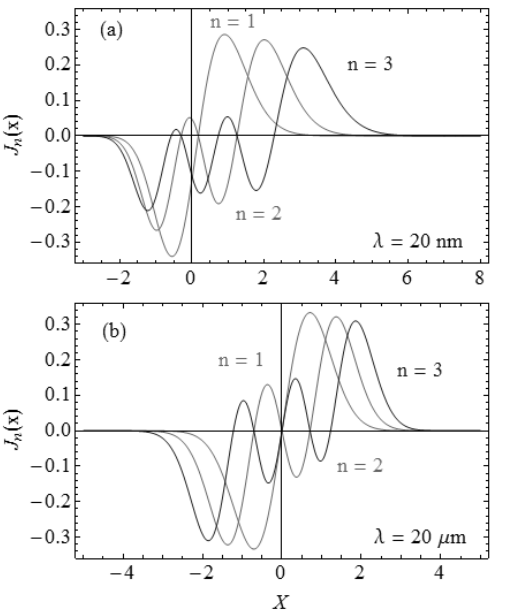

Figure 4. The same as Figure 2 but for probability current density $J_n(x)$ (in units of $\left[L_y\alpha_c(x_0)\right]^{-1/2}$)

5. Conclusions

In summary, we have investigated the Dirac electron system in gapped graphene under an exponentially decaying magnetic field by solving the Dirac-Weyl equations. Our results showed that

effective potential is independent of the structure of the system but of the type of magnetic field. The Landau-level structure is significantly different from the case of a uniform magnetic field: the number of Landau levels, in this case, is finite and is strongly dependent on the penetration depth of the magnetic field. We have also investigated the probability density and current density for each Landau level. It is expected that our results will motivate the study on the magneto-optical properties in the gapped graphene under inhomogeneous magnetic fields.

References

Cooper, F., Khare, A., & Sukhatme, U. (1995). Supersymmetry and quantum mechanics. *Physics Reports, 251*(5-6), 267-385. https://doi.org/10.1016/0370-1573(94)00080-M.

Eshghi, M., & Mehraban, H. (2017). Exact solution of the Dirac–Weyl equation in graphene under electric and magnetic fields. *Comptes Rendus Physique, 18*(1), 47-56. https://doi.org/10.1016/j.crhy.2016.06.002.

Ghosh, T. K. (2008). Exact solutions for a Dirac electron in an exponentially decaying magnetic field. *Journal of Physics: Condensed Matter, 21*(4), 045505. https://doi.org/10.1088/0953-8984/21/4/045505.

Handrich, K. (2005). Quantum mechanical magnetic-field-gradient drift velocity: An analytically solvable model. *Physical Review B, 72*(16), 161308. https://doi.org/10.1103/PhysRevB.72.161308.

Jiang, L., Zheng, Y., Li, H., & Shen, H. (2010). Magneto-transport properties of gapped graphene. *Nanotechnology, 21*(14), 145703. https://doi.org/10.1088/0957-4484/21/14/145703.

Krstajić, P., & Vasilopoulos, P. (2012). Integer quantum Hall effect in gapped single-layer graphene. *Physical Review B, 86*(11), 115432. https://doi.org/10.1103/PhysRevB.86.115432.

Kuru, Ş., Negro, J., & Nieto, L. (2009). Exact analytic solutions for a Dirac electron moving in graphene under magnetic fields. *Journal of Physics: Condensed Matter, 21*(45), 455305. https://doi.org/10.1088/0953-8984/21/45/455305.

Midya, B., & Fernández, D. (2014). Dirac electron in graphene under supersymmetry generated magnetic fields. *Journal of Physics A: Mathematical Theoretical, 47*(28), 285302. https://doi.org/10.1088/1751-8113/47/28/285302.

Novoselov, K. S., Geim, A. K., Morozov, S. V., Jiang, D., Katsnelson, M. I., Grigorieva, I. V., Dubonos, S., & Firsov, A. (2005). Two-dimensional gas of massless Dirac fermions in graphene. *Nature, 438*(7065), 197-200. https://doi.org/10.1038/nature04233.

Novoselov, K. S., Jiang, D., Schedin, F., Booth, T., Khotkevich, V., Morozov, S., & Geim, A. K. (2005). Two-dimensional atomic crystals. *Proceedings of the National Academy of Sciences, 102*(30), 10451-10453. https://doi.org/10.1073/pnas.0502848102.

Wang, D., & Jin, G. (2013). Effect of a nonuniform magnetic field on the Landau states in a biased AA-stacked graphene bilayer. *Physics Letters A, 377*(40), 2901-2904. https://doi.org/10.1016/j.physleta.2013.08.041.

Wang, D., Shen, A., Lv, J.-P., & Jin, G. (2019). Unique Landau-level structure of monolayer black phosphorus under an exponentially decaying magnetic field. *Journal of Physics: Condensed Matter, 32*(9), 095301. https://doi.org/10.1088/1361-648X/ab561a.